Letters on Materials 15 (4), 2025 pp. 388-393 www.lettersonmaterials.com

Received 14 November 2025; Accepted 26 November 2025 https://elibrary.ru/xopxwq
https://doi.org/10.48612/letters/2025-4-388-393

Dynamic recrystallization in a heavily alloyed PM γ+γ' nickel-based superalloy

R. I. Zainullin, R. V. Shakhov, Sh. Kh. Mukhtarov†, V. M. Imayev

†shamilm@imsp.ru

Institute for Metals Superplasticity Problems, Russian Academy of Sciences, Ufa 450001, Russia

Abstract: Effect of isothermal hot compression at temperatures below the γ' solvus temperature on the development of dynamic recrystallization was studied in a powder metallurgy (PM) γ+γ' nickel-based superalloy VV750P (ВВ750П, Ni-9.9(Al, Ti, Nb)-33.7(Co, Cr, Mo, W, Hf)-0.075(C, B) (wt.%)). This superalloy is heavily alloyed and has a high γ' solvus temperature (T_s=1190°C). In the initial HIPed condition, the average γ grain size was $d \approx 29$ μm and volume fraction of γ' (Ni_3(Al, Ti, Nb)) phase about 70%. Small cylindrical samples were prepared from the HIPed material and subjected to isothermal single-stage compression in the temperature range of 1125–1175°C ((T_s–65)–(T_s–15), where T_s is the γ' solvus temperature) with an initial strain rate $\dot{\varepsilon}=10^{-2}$ s^{-1} to an engineering strain ε=75%. The temperature/strain rate conditions were chosen on basis of previously performed studies on other PM nickel-based superalloys such as EP741NP (ЭП741НП) and VV751P (ВВ751П). In contrast to previously performed works, the present investigation aimed at achieving completely recrystallized and fine-grained structure without using annealing after HIP and intermediate recrystallization annealing. Hot compression at 1125–1175°C led to development of dynamic recrystallization. However, recrystallization kinetics significantly depended on deformation temperature. The fastest kinetics of recrystallization was reached during compression at 1175°C (T_s–15) that is only slightly below the γ' solvus temperature. In contrast to compression at 1125 and 1150°C, hot compression at 1175°C resulted in a complete disappearance of coarse prior γ grains and formation of completely recrystallized and fine-grained structure. Thus, single-stage isothermal hot forging of HIPed PM superalloy at a slightly subsolvus temperature without additional annealing can be considered as an alternative processing route instead of two- or three-stage forging at subsolvus temperatures with intermediate annealing.

Keywords: nickel-based superalloy, powder metallurgy, microstructure, γ' phase, hot deformation, dynamic recrystallization

Acknowledgements: *The present work was supported by the Russian Science Foundation (Grant No. 25-29-00806, https://rscf.ru/en/project/25-29-00806/). The work was performed using the facilities of the shared services center "Structural and Physical-Mechanical Studies of Materials" at the Institute for Metals Superplasticity Problems of Russian Academy of Sciences.*

1. Introduction

It is known that high-pressure discs and static parts for gas turbine engines are typically manufactured from powder metallurgy (PM) nickel-based superalloys using hot isostatic pressing (HIP) followed by heat treatment [1–5]. HIP is used to consolidate the powder into a dense and near-net-shaped part, while the heat treatment is carried out to optimize the microstructure and mechanical properties for high-temperature application. However, this convenient and relatively inexpensive processing route has some drawbacks. The fact is that PM superalloys can have microstructural heterogeneities associated with the original powder particle surfaces, commonly referred to as prior particle boundaries (PPBs). These boundaries often accumulate various secondary phases, such as γ' precipitates, oxides, oxy-carbides, and carbides (e.g., MC, M_6C), which can deteriorate mechanical properties [6–10]. One approach to exclude or minimize the detrimental influence of PPBs is supersolvus solution heat treatment, wherein the superalloy is heated above the γ' solvus temperature to dissolve detrimental precipitates and activate grain boundary migration [9,11]. However, this approach can induce significant grain growth due to the high temperatures leading to worsening of mechanical properties [12]. To eliminate the detrimental effect of PPB precipitates and improve mechanical properties, an effective approach is to forge the HIP-consolidated material. This process promotes dynamic recrystallization leading to grain refinement, facilitates the breakup and more uniform redistribution of PPBs throughout the structure, thereby improving the overall performance characteristics of the material.

In our recent works [13–17], it was shown that hot forging with intermediate annealing at subsolvus temperatures (in the range of (T_s–70)–(T_s–25), where T_s is the γ' solvus temperature) is the most favorable for the development of recrystallization processes in heavily alloyed nickel-based superalloys, produced both by ingot and powder metallurgy. Before forging, the material was always subjected to annealing at around γ' solvus temperature followed by slow controlled cooling to cause coalescence of the γ' phase, thereby facilitating the development of recrystallization [13–20]. However, the processing route including preliminary annealing, multi-stage forging with intermediate recrystallization annealing is very labor-intensive and time consuming. From a practical point of view, it would be reasonable to achieve coalescence of the γ' phase already at the HIP stage, and to carry out the forging procedure in one stage without intermediate annealing.

The present work was aimed at achieving a homogeneous and fine-grained structure in a heavily alloyed PM nickel-based superalloy VV750P (ВВ750П) using single-stage hot compression under isothermal conditions without using intermediate recrystallization annealing. The as-received PM superalloy was produced by HIP followed by controlled slow cooling, which ensured the coalescence of the γ' phase and thus increased the dislocation glide distance promoting the development of recrystallization. The hot compression was performed at subsolvus temperatures with a strain rate, which was earlier defined as an optimal one. Potential advantages of the single-stage forging for obtaining tailored microstructure in high-pressure discs are discussed.

2. Material and methods

The as-received billets of the VV750P superalloy were produced using the following processing steps: (i) the vacuum-induction melting of a cylindrical ingot followed by its dispersion into granules; (ii) the plasma-arc melting and centrifugal sputtering of a rapidly rotating cast electrode via the Plasma Rotating Electrode Process (PREP) yielding spherical granules 50–100 μm in diameter; (iii) HIP of the granules in a steel capsule, followed by slow controlled cooling in a furnace. Table 1 presents the nominal composition of the VV750P superalloy [21], which was verified by energy dispersive X-ray spectroscopy (EDS).

To determine the γ' solvus temperature, quenching experiments followed by microstructural examination were conducted. Full dissolution of the coarse primary γ' phase was obtained after quenching from 1190°C and therefore the γ' solvus temperature for assumed as $T_s \approx 1190$°C.

Cylindrical samples with a size of ∅8×12 mm were cut from the as-received billet. Compression tests were carried out under isothermal conditions at 1125–1175°C (in the range of $(T_s-65)-(T_s-15)$, where T_s is the γ' solvus temperature) with an initial strain rate of $\dot{\varepsilon}=10^{-2}$ s^{-1} to an engineering strain of $\varepsilon \approx 75\%$ ($e \approx 1.4$). As mentioned, the strain rate of $\dot{\varepsilon}=10^{-2}$ s^{-1} was earlier defined as an optimal one for different PM nickel-based superalloys [14,16–18,20]. The compression tests were used to plot the true stress-engineering strain curves taking into account the graduate increase of the cross section of samples during compression. The stress-strain curves were plotted up to the engineering strain $\varepsilon \approx 40\%$.

Scanning electron microscopy (SEM) in backscattering and secondary (BSE, SE) electron mode and electron backscatter diffraction (EBSD) analysis were carried out to characterize the microstructure. EBSD analysis was performed using the CHANNEL 5 software with a scan step size of 0.5 μm. The obtained normal-direction EBSD maps (presented as inverse pole figures or IPF) took into consideration the γ grains and coarse primary γ' phase located along the γ grain boundaries, whereas the fine secondary intragranular γ' precipitates formed during cooling of the deformed samples were not distinguished on the IPF maps. Besides IPF maps, Kernel average misorientation (KAM) maps, EBSD grain boundary maps and grain orientation spread (GOS) maps were also drawn. Grain/interphase boundaries were believed high-angle ones if their misorientation angle exceeded 15°. The EBSD data were used to determine the average size of γ grains/primary γ' phase with high-angle boundaries. Before SEM examination, the surfaces of the samples were subjected to mechanical polishing and short-term (for about 10 s) electrolytic polishing.

3. Results and discussion

Figure 1 shows the BSE and SE images the VV750P superalloy in the initial HIPed condition. The microstructure was uniform and had an average γ grain size of $d \approx 29$ μm (Fig. 1a, b). The coarse primary γ' phase, 2–5 μm in size, was located along the grain boundaries (Fig. 1c). Its volume

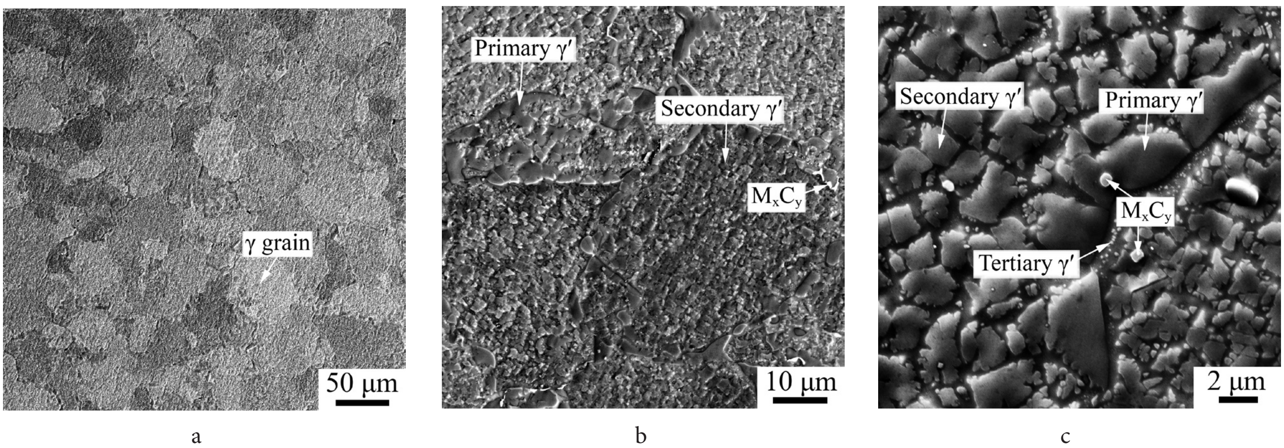

Fig. 1. SEM images of the VV750P superalloy in the initial HIPed condition: BSE (a, b), SE (c).

Table 1. Chemical composition of the VV750P superalloy (in wt.%).

	Ni	Al	Ti	Nb	Cr	Co	W	Mo	Hf	C	B
Nominal	bal.	3.4–4	3.5–3.9	1.6–2	9–11	14–16	5.4–6.2	3–3.6	<0.1	<0.08	0.015
Measured	-	4.0	3.9	2.0	9.7	14.6	6.2	3.1	-	-	-

fraction was about 15%. The secondary γ' precipitates had a size of 1–2 μm. Between primary and secondary γ' tertiary γ' precipitates with a size of less than 0.1 μm were sometimes distinguished. The volume fraction of primary and secondary γ' phase was estimated at approximately 70%. There were also light carbide particles with a size of 0.5–2 μm. Their volume fraction did not exceed 1%.

Figure 2 represents the true stress-engineering strain curves obtained as a result of compression tests of samples at different temperatures. With increasing the test temperature, the flow stress decreased, which is associated with dissolution of the γ' phase and an increase in the dislocation glide distance. During deformation at 1125 and 1150°C ((T_s-65)–(T_s-40)), the flow stress first increased reaching peak values at $\varepsilon=5-10\%$ and then decreased, which indirectly indicates the development of dynamic recovery and recrystallization. During deformation at 1175°C (T_s-15), the flow stress first increased reaching the maximum at $\varepsilon\approx10\%$ and then very slightly decreased becoming almost constant after $\varepsilon=30\%$. There are two possible explanations for why the flow stress changes very little during compression at 1175°C. In the first case, the plastic deformation occurs under superplastic or near superplastic conditions, so the rates of dislocation generation and annihilations due to grain boundary sliding are almost the same ensuring approximate equal strengthening and softening during deformation. In this case, the γ grain size should not change after compression. In the second case, the plastic deformation leads to rapid occurrence of recrystallization and simultaneous growth of recrystallized γ grains (due to the low volume fraction of the γ' phase), followed by the re-accumulation of dislocations in these grains. This scenario should lead to microstructural refinement due to dynamic recrystallization with the simultaneous establishment of an equilibrium between grain refinement and coarsening. To elucidate the microstructural changes after compression, EBSD analysis was carried out.

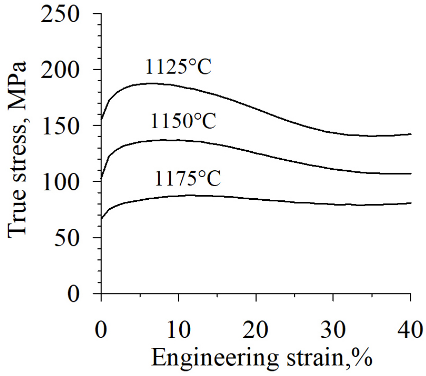

Fig. 2. True stress-engineering strain curves obtained during compression of superalloy samples at various temperatures ($\dot{\varepsilon}=10^{-2}$ s^{-1}).

Figures 3–5 demonstrate the results of EBSD analysis of the superalloy after hot compression at 1125–1175°C. It is seen that hot compression at 1125 and 1150°C ((T_s-65)–(T_s-40)) led to the formation of refined partially

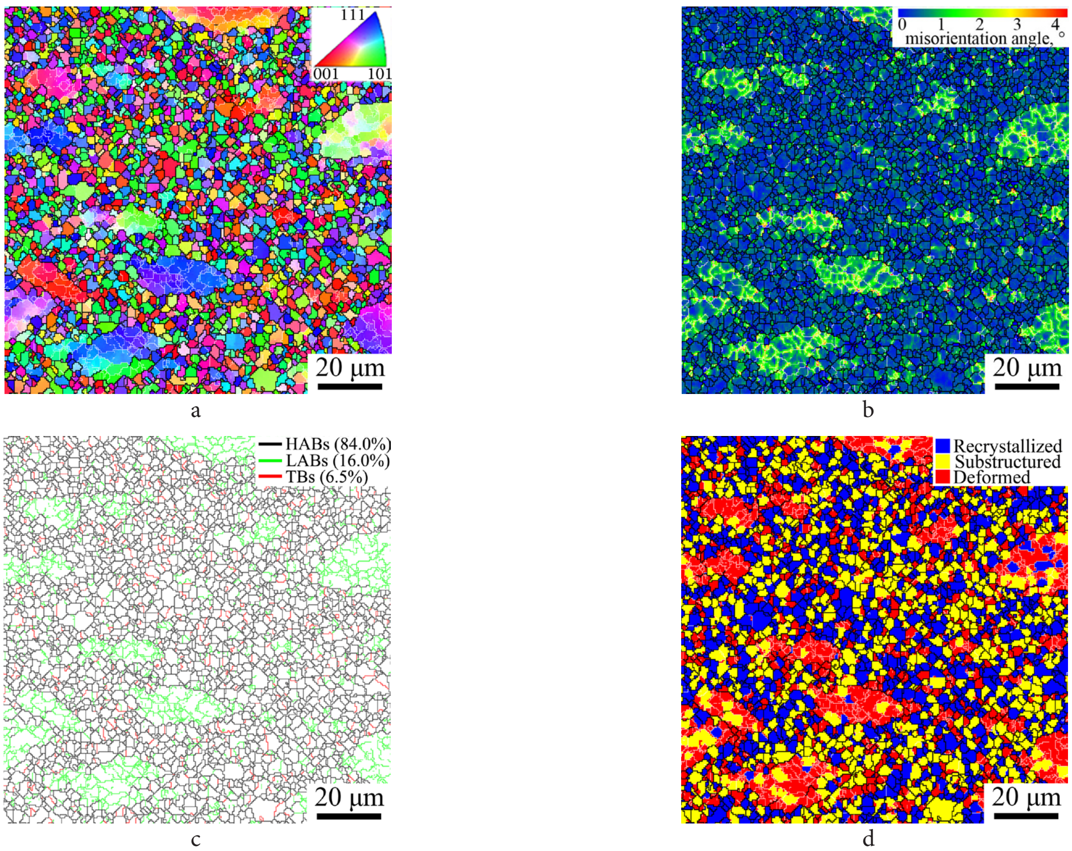

Fig. 3. (Color online) IPF (inverse pole figure) map (a), corresponding KAM map (b), grain boundary map (c) and GOS (grain orientation spread) map (d) obtained for the HIPed VV750P superalloy subjected to compression at T=1125°C ($\dot{\varepsilon}=10^{-2}$ s^{-1}, $e\approx1.4$): (a) low- and high-angle grain/interphase boundaries are indicated by white and black lines, respectively, (b) the green color shows areas with a higher dislocation density, (c) black, green and red lines show high-angle, low-angle and twin boundaries, respectively, (d) HAB, LAB and TB means high-angle, low-angle and twin boundaries, respectively. The deformation axis is vertical.

recrystallized microstructures with a fairly high proportion of high-angle grain/interphase boundaries. Besides, coarse non-recrystallized γ grains elongated along the material flow remained after compression. These coarse non-recrystallized grains are visible in the KAM maps as containing a higher dislocation density (Figs. 3b and 4b). In the GB maps and GOS maps, these grains are visible as containing low-angle boundaries and as deformed grains, respectively (Figs. 3c and 4c). Twin boundaries (Σ3) were formed during cooling immediately after compression tests.

The average size of recrystallized γ grains/primary γ' phase with high-angle boundaries (excluding coarse non-recrystallized γ grains) after compression at 1125 and 1150°C was $d \approx 2$ and 2.6 μm, respectively. With increasing the test temperature from 1125 to 1150°C the fraction of high-angle boundaries increased from 84 to 89.4% and the fraction of coarse non-recrystallized grains decreased. Thus, softening during compression at 1125 and 1150°C is explained by dynamic recovery and recrystallization, while the volume fraction of the recrystallized microstructure turned out to be far from 100%.

Hot compression at 1175°C (T_s−15) resulted in disappearance of coarse non-recrystallized γ grains and formation of fully recrystallized microstructure with a high proportion (88%) of high-angle grain/interphase boundaries (Fig. 5). Twin boundaries (Σ3) formed during cooling immediately after compression were also observed. Their fraction was higher than after compression at 1125 and 1150°C, which can be ascribed to higher temperature. Generally, the formation of twin boundaries is associated with a low stacking fault energy in the nickel-based superalloys. The average size of γ grains/primary γ' phase with high-angle boundaries was defined as $d \approx 4.3$ μm. Apparently, dissolution of the γ' phase at 1175°C increased the dislocation glide distance, which promoted the development of dynamic recrystallization. Migration of grain/interphase boundaries simultaneously occurred leading to grain growth and a decrease in dislocation density. As follows from Fig. 2, approximate equilibrium between dislocation generation and dislocation disappearance due to dynamic recovery, recrystallization and grain growth was reached during compression at 1175°C. It is worth noting that the PPBs were not distinguished after hot compression at 1125–1175°C.

In our previous works [13,20], it was shown that continuous dynamic recrystallization was the main recrystallization mechanism in a heavily alloyed nickel-based superalloy manufactured by ingot-metallurgy, while discontinuous dynamic recrystallization was the dominant recrystallization mechanism in the case a heavily alloyed PM nickel-based superalloy in the course of hot deformation at subsolvus temperatures under optimized temperature/strain rate conditions. The present work suggests that optimized temperature/strain rate conditions of hot deformation ($T = T_s$−15, $\dot{\varepsilon} = 10^{-2}$ s^{-1}, $e \approx 1.4$) provided the development of both discontinuous and continuous dynamic recrystallization and, it seems, only the action of both of these mechanisms

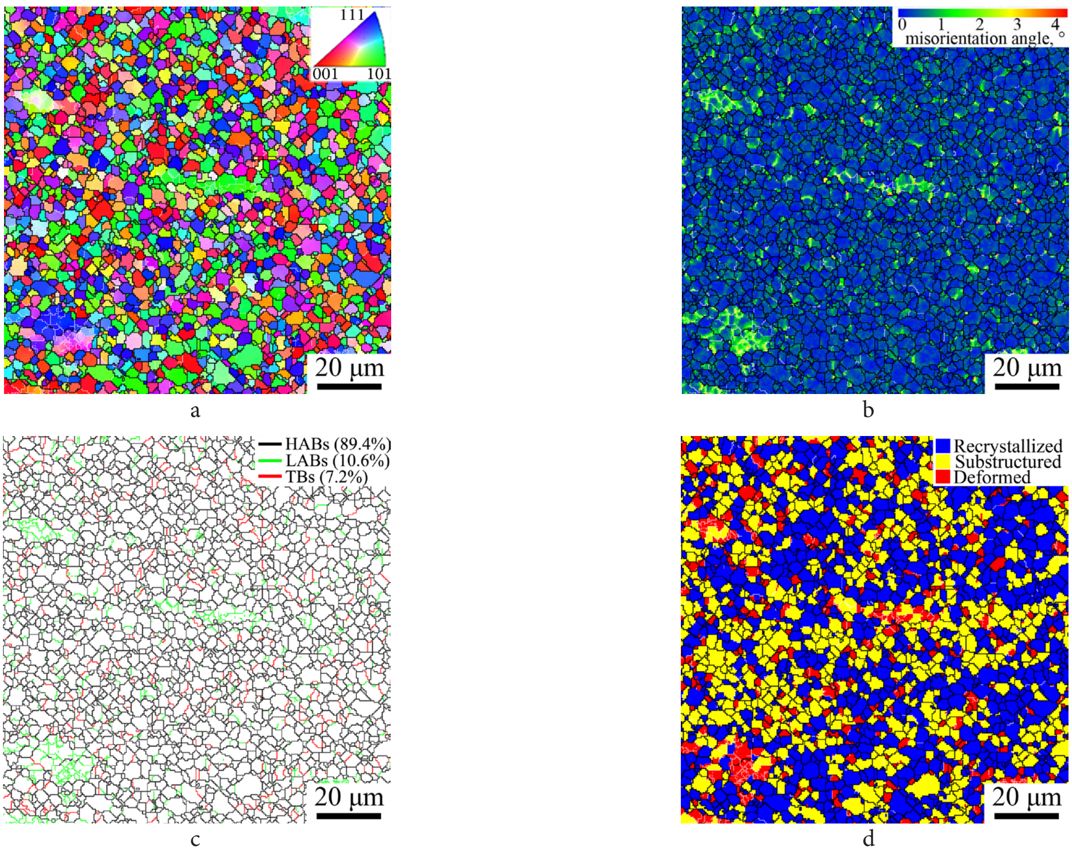

Fig. 4. (Color online) IPF (inverse pole figure) map (a), corresponding KAM map (b), grain boundary map (c) and GOS (grain orientation spread) map (d) obtained for the HIPed VV750P superalloy subjected to compression at T=1150°C ($\dot{\varepsilon}$=10^{-2} s^{-1}, $e \approx 1.4$): (a) low- and high-angle grain/interphase boundaries are indicated by white and black lines, respectively, (b) the green color shows areas with a higher dislocation density, (c) black, green and red lines show high-angle, low-angle and twin boundaries, respectively, (d) HAB, LAB and TB means high-angle, low-angle and twin boundaries, respectively. The deformation axis is vertical.

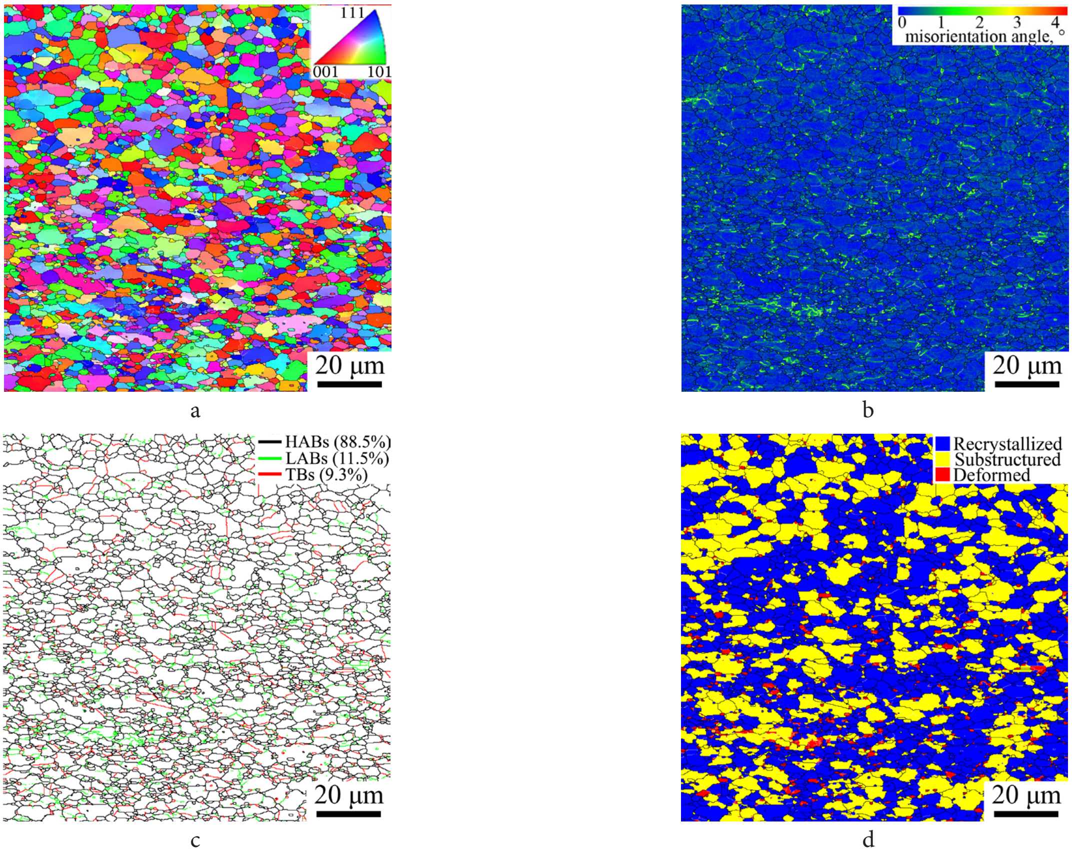

Fig. 5. (Color online) IPF (inverse pole figure) map (a), corresponding KAM map (b), grain boundary map (c) and GOS (grain orientation spread) map (d) obtained for the HIPed VV750P superalloy subjected to compression at T=1175°C ($\dot{\varepsilon}$=10^{-2} s^{-1}, e≈1.4): (a) low- and high-angle grain/interphase boundaries are indicated by white and black lines, respectively, (b) the green color shows areas with a higher dislocation density, (c) black, green and red lines show high-angle, low-angle and twin boundaries, respectively, (d) HAB, LAB and TB means high-angle, low-angle and twin boundaries, respectively. The deformation axis is vertical.

led to the formation of a completely recrystallized microstructure. This statement, however, needs additional experimental verification. At the same time, discontinuous dynamic recrystallization was apparently the dominant recrystallization mechanism during hot compression of samples of the VV750P superalloy during deformation at 1125 and 1150°C.

Thus, the experiments demonstrated that isothermal hot working at a subsolvus temperature (just slightly below the γ' solvus temperature) is highly effective for the development of dynamic recrystallization in a heavily alloyed nickel-based superalloy produced by HIP without annealing both before forging (to promote γ' phase coalescence) and during forging procedure (to promote recrystallization). However, it appears to effective only when HIP is followed by slow controlled cooling to provide sufficient dislocation glide distance for the development of dynamic recrystallization. It is worth noting that the PPBs were excluded by isothermal hot compression.

The performed experiments allow us thus to consider single-stage isothermal hot forging of the HIPed PM superalloy at a slightly subsolvus temperature as an alternative processing route instead of two- or three-stage forging at subsolvus temperatures with intermediate annealing, which we typically applied for PM heavily alloyed nickel-based superalloys [14,16–18,20]. No doubt that single-stage isothermal forging is much more cost effective than multistage forging and therefore can be used for obtaining tailored microstructure for instance in turbine discs for gas turbine engines. Note that a gradient microstructure, which is typically desirable in a turbine disc, can be reached in this case via special heat treatment in a gradient temperature field [22–24].

4. Conclusions

The present work was devoted to study of dynamic recrystallization in a heavily alloyed PM nickel-based superalloy VV750P intended for use as a structural material in gas turbine engines. The following main conclusions can be drawn:

– The isothermal hot deformation at T=1125–1150°C ($\dot{\varepsilon}$=10^{-2} s^{-1}, e≈1.4), that is in the range of (T_s–65)–(T_s–40), where T_s is the γ' solvus temperature, led to intensive occurrence of dynamic recovery and recrystallization. However, such deformation did not provide the formation of refined and completely recrystallized microstructure.

– Optimal conditions of isothermal hot deformation were defined as T=1175°C ($\dot{\varepsilon}$=10^{-2} s^{-1}, e≈1.4), that is just slightly below the γ' solvus temperature (T_s–15). Microstructural analysis revealed that the uniform and completely recrystallized fine-grained structure was achieved after deformation at 1175°C. Presumably, this was due to the fact, that both discontinuous and continuous dynamic recrystallization occurred under these conditions. A feature of dynamic recrystallization at 1175°C was extensive development and simultaneous migration of grain/interphase boundaries leading to some grain growth.

– The performed experiments show that there is no strict need to carry out annealing both before forging (to promote the coalescence of the γ' phase) and during forging procedure (to promote recrystallization) for complete recrystallization of the microstructure in the case of a heavily alloyed nickel-based superalloy when using slow controlled cooling after HIP, which provides sufficient dislocation glide distance for the development of dynamic recrystallization.

References

1. J. Radavich, D. Furrer, Assessment of Russian P/M superalloy EP741NP, Superalloys 2004 (2004) 381–390.
2. L. B. Ber, S. V. Rogozhkin, A. A. Khomich, A. G. Zaluzhnyi, Distribution of Alloying Element Atoms between γ- and γ'-Phase Particles in a Heat-Resistant Nickel Alloy, Phys. Metals Metallogr. 123 (2022) 163–177.
3. C. Qiu, Net-Shape Hot Isostatic Pressing of a Nickel-Based Powder Superalloy: Ph. D. thesis, University of Birmingham, U. K., 2010, 295 p.
4. G. Raisson, J. Y. Guédou, D. Guichard, J. M. Rongvaux, Production of Net-Shape Static Parts by Direct HIPing of Nickel Base Superalloy Prealloyed Powders, Adv. Mat. Res. 278 (2011) 277–282.
5. J. H. Moll, J. J. Conway, Characteristics and Properties of As-HIP P/M Alloy 720, Superalloys 2000 (2000) 135–142.
6. J. Bai, Q. Lin, G. Tian, J. Zou, T. A. Dean, Review and Analysis of Powder Prior Boundary (PPB) Formation in Powder Metallurgy Processes for Nickel-based Super Alloys, J. Powder Metall. Min. 04 (2015) 1000127.
7. C. Qiu, X. Wu, J. Mei, P. Andrews, W. Voice, Influence of heat treatment on microstructure and tensile behavior of a hot isostatically pressed nickel-based superalloy, J. Alloys Compd. 578 (2013) 454–464.
8. J. Hou, J.X. Dong, Z.H. Yao, H. Jiang, M.C. Zhang, Influences of PPB, PPB affect zone, grain boundary and phase boundary on crack propagation path for a P/M superalloy FGH4096, Mater. Sci.Eng. A 724 (2018) 17–28.
9. L. Chang, W. Sun, Y. Cui, R. Yang, Preparation of hot-isostatic-pressed powder metallurgy superalloy Inconel 718 free of prior particle boundaries, Mater. Sci.Eng. A 682 (2017) 341–344.
10. C. Cai, K. Pan, Q. Teng, X. Gao, B. Song, J. Liu, Q. Wei, K. Zhou, Y. Shi, Simultaneously enhanced strength and ductility of FGH4097 nickel-based alloy via a novel hot isostatic pressing strategy, Mater. Sci. Eng. A 760 (2019) 19–25.
11. C. L. Qiu, M. M. Attallah, X. H. Wu, P. Andrews, Influence of hot isostatic pressing temperature on microstructure and tensile properties of a nickel-based superalloy powder, Mater. Sci. Eng. A 564 (2013) 176–185.
12. G. A. Rao, M. Srinivas, D. S. Sarma, Effect of solution treatment temperature on microstructure and mechanical properties of hot isostatically pressed superalloy Inconel* 718, Mater. Sci. Technol. 20 (2004) 1161–1170.
13. S. K. Mukhtarov, V. M. Imayev, A. V. Logunov, Y. N. Shmotin, A. M. Mikhailov, R. A. Gaisin, R. V. Shakhov, A. A. Ganeev, R. M. Imayev, Recrystallisation behaviour and mechanical properties of a novel Re-containing nickel-base superalloy, Mater. Sci. Technol. 36 (2019) 1605–1613.
14. A. A. Ganeev, V. A. Valitov, F. Z. Utyashev, V. M. Imaev, Effect of Thermomechanical Treatment on the Formation of Gradient Structure and Mechanical Properties in a Disk Made of Powder-Metallurgy Nickel-Based Superalloy, Phys. Met. Metallogr. 120 (2019) 410–416.
15. V. Imayev, S. Mukhtarov, K. Mukhtarova, A. Ganeev, R. Shakhov, N. Parkhimovich, A. Logunov, Influence of Forging and Heat Treatment on the Microstructure and Mechanical Properties of a Heavily Alloyed Ingot-Metallurgy Nickel-Based Superalloy, Metals 10 (2020) 1606.
16. R. I. Zainullin, S. K. Mukhtarov, A. A. Ganeev, R. V. Shakhov, V. M. Imayev, Effect of hot forging on formation of a fine-grained structure and mechanical properties of a powder metallurgy nickel base superalloy, Lett. Mater. 13 (4) (2023) 414–419. DOI: 10.22226/2410-3535-2023-4-414-419 Webpage
17. S. Mukhtarov, D. Karyagin, A. Ganeev, R. Zainullin, R. Shakhov, V. Imayev, The Effect of Forging and Heat Treatment Variables on Microstructure and Mechanical Properties of a Re-Bearing Powder-Metallurgy Nickel Base Superalloy, Metals 13 (2023) 1110.
18. S. K. Mukhtarov, D. A. Karyagin, A. V. Logunov, A. A. Ganeev, R. I. Zainullin, R. V. Shakhov, V. M. Imayev, Effect of hot working on the microstructure and tensile properties of a novel PM Re-bearing nickel base superalloy, Lett. Mater. 12 (2022) 457–462.
19. Sh. Mukhtarov, R. Shakhov, A. Ganeev, V. Imayev, Effect of direct ageing on the microstructure, tensile properties and fracture behavior of a Re-bearing polycrystalline nickel-based superalloy, Mater. Sci. Technol. (2025) in press.
20. R. I. Zainullin, Sh. Kh. Mukhtarov, R. V. Shakhov, A. A. Ganeev, V. M. Imayev, Effect of Forging and Heat Treatment on Microstructure and Mechanical Properties of a PM Nickel-Based Superalloy, J. Mater. Eng. Perform. (2025) in press.
21. GOST R 52802-2007, Granulated heat-resistant nickel alloys. Grades. (in Russian)
22. Y. Ning, Z. Yao, H. Guo, M. W. Fu, Structural-gradient-materials produced by gradient temperature heat treatment for dual-property turbine disc, J. Alloys Compd. 557 (2013) 27–33.
23. J. Gayda, Dual Microstructure Heat Treatment of a Nickel-Base Disk Alloy, NASA/TM-2001-211168. Available online
24. R. J. Mitchell, J. A. Lemsky, R. Ramanathan, H. Y. Li, K. M. Perkins, L. D. Connor, Process development & microstructure & mechanical property evaluation of a dual microstructure heat treated advanced nickel disc alloy, Superalloys 2008 (2008) 347–356.